JOURNAL OF MATERIALS SCIENCE 33 (1998) 2905–2917

Water induced anelasticity of porous media

J. LEPAGE
Laboratoire de Science et Génie des Surfaces, LSGS, URA 1402 CNRS, Ecole des Mines, Parc de Saurupt, 54042 Nancy Cédex, France

J. MENAUCOURT
Laboratoire de Chimie Physique pour l'Environnement, LCPE, UMR 9992 CNRS, Université Henri Poincaré-Nancy I, 405 rue de Vandoeuvre, 54600 Villers-les-Nancy, France

The anelastic behaviour of some porous media has been studied as a function of their water content. The investigated systems (oxides, calcite, carbon) have been chosen to provide various chemical as well as physical environments to the fluid. From the chemical point of view, the hydrophilic/hydrophobic balance has been considered. The hydrophilic character of the oxides has been varied by heat treatments. Naturally hydrophobic graphite has been made hydrophilic by oxidation. The experimental results point to the large influence of the first water monolayer on the anelastic properties of the composite media. The main physical character taken into account is the crack aspect ratio i.e. the ratio of the smallest to largest dimension of the pores. Two models have been considered. In the first one anelasticity results from the molecular motion of the adsorbate inside the fluid phase. The second one is a grain-to-grain contact model which takes into account the known variations of the coefficient of friction with hydration of the surfaces. The physical state of water in the low content range is discussed: it is conjectured to be liquid. The maximum in the damping efficiency of the composite as the water content is varied is still a matter of debate.

1. Introduction

Viscoelastic properties of non-metal materials such as paper, carbons, polymers, clays and rocks are known to be moisture-sensitive. The obvious cause of the phenomenon is adsorption of water vapour from the atmosphere on the inner surfaces of the solids. In a previous study on the anelastic properties of porous silica glass as a function of water vapour adsorption, the breaking of H-bonds has been found to be the main cause of anelasticity [1]. The purpose of this work reported here is to test if mechanisms worked out on Vycor are relevant to other materials. The main conclusions of this previous work are listed below. Physisorbed water H-bonds to surface silanols or other polar species. At a relative humidity (RH) of 60%, statistically, each hydroxyl is covered by a water molecule. On hydroxylated silica the rate of change of Young's modulus and damping factor against the water content X, $\mathrm{d}E/\mathrm{d}X$ and $\mathrm{d}Q^{-1}/\mathrm{d}X$ are positive in the monolayer range and nil beyond.

On dehydroxylated silica the rate of change of Young's modulus $\mathrm{d}E/\mathrm{d}X$ is negative but the damping factor $\mathrm{d}Q^{-1}/\mathrm{d}X$ is still positive in the monolayer range and nil beyond. High temperature annealing favours siloxane bridge at the expense of silanols, which results in higher Young's modulus and quality factor. Results on attenuation are condensed into the analytic expression

$$Q^{-1} = Q_0^{-1} + k_1[\mathrm{OH}][\mathrm{H_2O}] + k_2[\mathrm{OH}_\alpha]^2 \quad (1)$$

The term $k_1[\mathrm{OH}][\mathrm{H_2O}]$ describes H-bonding between water molecules physisorbed in the first layer and the chemisorbed silanols, which is assumed to be a relaxation species. It takes into account the linearity of the $Q^{-1}(X)$ curve frequently observed during adsorption below the monolayer coverage, where [OH] is constant [2]. The subscript α in the term $k_2[\mathrm{OH}_\alpha]^2$ indicates that the silanols active in damping are H-bonded silanols desorbing in the 200–450 °C range on silica while isolated silanols desorbing beyond 500 °C are inactive in the damping process. It accounts for the dependence of $Q^{-1}(X)$ on vacuum annealing prior to experiment [2]. The assumed quadratic dependence of $Q^{-1}(X)$ on $[\mathrm{OH}_\alpha]$ has only theoretical grounds (the number of H bonds is proportional to the square of the concentration) and up to now has not been experimentally studied. This paper is devoted to a discussion of the validity of these concepts. To test them and get further insights into the subject, the range of the materials tested has been extended, including natural as well as synthetic materials.

2. Experimental methods

The composite Young's modulus E and damping factor Q^{-1} of porous materials are measured by dynamic flexural bending of slender bars. Typical dimensions of the samples are length, $l = 100$ mm, thickness $h = 5$ mm and width $w = 10$ mm. E is given by the

0022–2461

classic formula

$$E = \frac{48\pi^2 l^4 \rho f_{ri}^2}{A_i^2 h^2} \quad (2)$$

where ρ is the specific mass of the sample, f_{ri} the frequency resonance of mode i and A_i a tabulated constant. The mass of the sample, and thus the water content, was determined by weighing after each vibratory test. During an experiment, only ρ, f_{ri} and E change and examination of Equation 2 shows that E varies as ρf_{ri}^2. The anelasticity of a material can be described by various interrelated parameters such as the logarithmic decrement of free vibrations λ, the loss angle $\tan\delta = E'/E''$ where E' and E'' are the real and imaginary parts of the complex Young's modulus or the quality factor Q. In these experiments the damping properties of the materials are characterized by the attenuation coefficient Q^{-1} which is given by

$$Q^{-1} = \frac{f_{ri}}{\Delta f} \quad (3)$$

where Δf is the bandwith of the resonance peak at -3 db. On high quality factor material such as Vycor, the third overtone has been used to improve the precision, on low Q materials the first one may be used. The water content of the sample is measured by X, ratio of the actual mass of the sample to the mass of the sample after extensive drying at 150 °C. $X > 1$ indicates adsorption of molecular water whilst $X < 1$ indicates dehydroxylation. Specific surface area are measured by the Brunauer–Emmett–Teller (BET) method at 77 K, using krypton as a probe molecule. Further experimental details are given in [1].

The investigated materials have been chosen in order to cover the widest span in the properties of interest, porosity ϕ, specific surface area A_s, hydrophilic versus hydrophobic character, structure of the porous phase, i.e. round versus sheet-like pores, mean pore diameter. These are silica (Vycor, a porous silica glass from Corning), calcite (natural chalk from Champaign, France), alumina and magnesia (porous alumina Al 25 and porous magnesia Mg25 from Degussa), granite from Neuvy-Bois quarry (Vendée, France) low density electro-graphite EG 319 P from Le Carbone Lorraine and mordenite, a high silica containing zeolite from Hungary. The physical characteristics of interest are gathered in Table I and described in more detail in Section 2.

3. Experimental results

3.1. Vycor

Variations of Young's modulus E and attenuation factor Q^{-1} as a function of the water content X have already been published [1], they are presented once again in Figs 1 to 3 for completeness. In the range $1 < X < 1.05$ swept during gentle drying up to 150 °C the mass change results from dehydration of the sample. In the range $0.98 < X < 1$ swept by heating under vacuum up to 650 °C dehydroxylation takes place according to the silanol condensation reaction

$$2\text{Si–OH} \longrightarrow \text{Si–O–Si} + \text{H}_2\text{O} \quad (4)$$

The changes in Young's modulus presented in Fig. 1 have been attributed to H-bonding of water molecules at $X > 1$ and to the formation of siloxane bonds according to Equation 4 at $X < 1$ [1]. Results in Fig. 2 show that between $X = 1.05$ and $X = 1.20$, no measurable changes in $Q^{-1}(X)$ can be noticed, however the mean value depends on the temperature of the previous annealing treatment, i.e. on the state of hydroxylation of the inner surfaces. The corresponding decrease is taken into account by the term $k_2[\text{OH}_\alpha]^2$ in Equation 1. It is shown in Fig. 3 that the OH species desorbing at temperature higher than 500 °C are inactive in the process of attenuation. The ordinate of the first point on the curve is the same, whatever is the hydroxyl content of the surface. Furthermore, the initial parts of the curves on Fig. 3 run parallel to themselves, which is indicative that [OH] is not rate limiting in the first term of Equation 1. At the highest temperature investigated, 750 °C, there are still enough geminal hydroxyls to H-bond to water during subsequent adsorption. These results are at variance with those obtained on quartz where a concentration of 6×10^{-4} at H decreases Q from 5×10^6 [3] to 1×10^6 [4]. In Vycor samples, because of porosity, Q is

TABLE I Relevant physical parameters of the materials under study

	Chemical composition	Mean porosity (%)	Mean pore diameter	BET surface area A_s ($m^2\,g^{-1}$)	Maximum water content ($g\,g^{-1}$)	Ratio of YM[a]
Vycor	SiO_2	28	2 nm	200	0.25	17/70
Chalk	$CaCO_3$	15	200 nm	2	0.15	
Alumina	Al_2O_3	25	25 μm	0.2	0.06	80/320
Magnesia	MgO	25	25 μm	0.2	0.07	120/340
Graphite	Pure carbon	depends on oxidation $30 \rightarrow 50$		Depends on oxidation $45 \rightarrow 12$	Depends on oxidation $0 \rightarrow 0.10$	12/80
Granite	SiO_2 75% Al_2O_3 14% (Na + K) 8% other oxides: balance	< 0.1	Fissural porosity	< 0.1	0.0005 $\rightarrow 0.007$ according to thermal treatments	
Mordenite	(Na_2,K_2,Ca) $[Al_2Si_{10}O_{24}]\ 7H_2O$	25	0.7 nm	300	0.23	

YM = Young's modulus.
[a] The ratio of the Young's modulus of the porous sample to the Young's modulus of the material at theoretical density, when known.

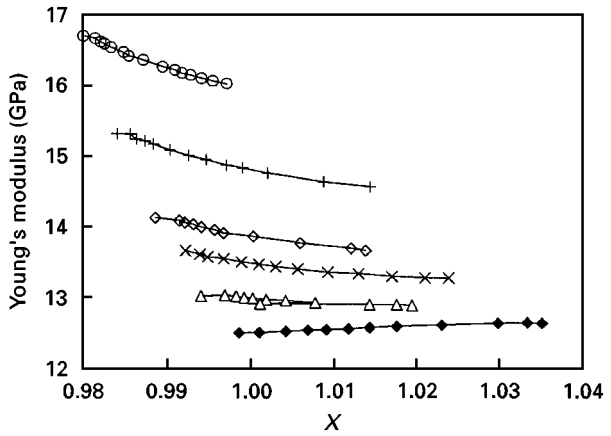

Figure 1 Young's modulus of Vycor glass during adsorption of water vapour from the laboratory air after annealing under vaccum at different temperatures. On Vycor which specific surface area is $200\,m^2\,g^{-1}$ a water monolayer corresponds to $\triangle X = 3 \times 10^{-2}$. (○) 650 °C; (+) 550 °C; (◇) 450 °C; (×) 400 °C; (△) 300 °C; (◆) 200 °C.

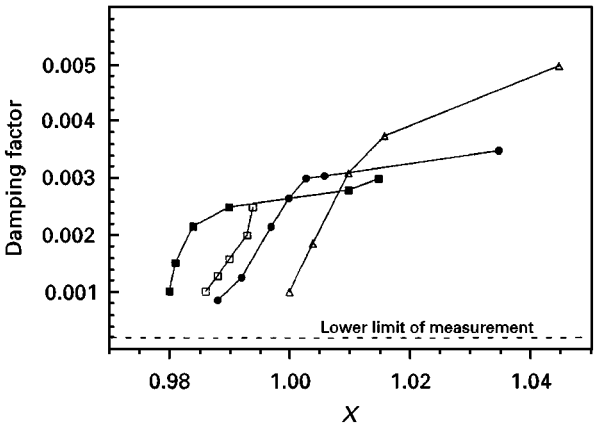

Figure 3 Attenuation of the first flexural mode of vibration of Vycor samples during adsorption of water vapour from the laboratory air after annealing under vacuum at the indicated temperatures. (■) 750 °C; (□) 550 °C; (●) 400 °C; (△) 200 °C.

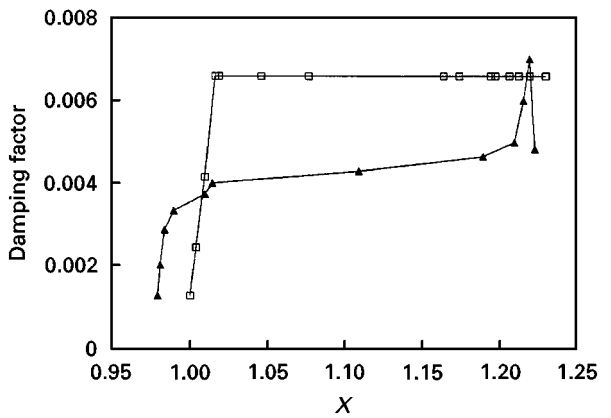

Figure 2 Attenuation of the first flexural mode of vibration of water soaked Vycor during drying: (□) pristine sample; (▲) after heat treatment at 650 °C under vacuum.

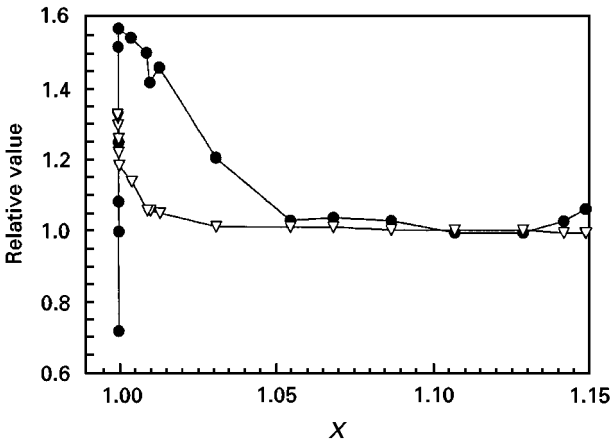

Figure 4 Q_0/Q (●), E/E_0 (▽) of chalk as a function of the water content during drying.

not higher than 5×10^3 (the higher Q measurable with the experimental apparatus working in air is 10^4). The Q investigated in this study are definitively lower than these values and the operative mechanisms are probably not the same. The most convincing proof of this assertion being the constancy of attenuation during high temperature dehydroxylation. Bulk mechanisms such as dislocation glide or climb or the so-called $4H_{(Si)}$ defect which are invoked to explain results in quartz [3] are not operative in porous silica.

The results obtained in [1] are in agreement with models recently appeared in the literature. Murphy [5], Spencer [6] and Bourbié *et al.* [7] have postulated that on hydrophilic samples attenuation results from the breaking of H-bonds between water molecules and surface silanols during the passage of the deformation wave and of the re-forming of these bonds out of phase. Damping of mechanical vibrations by adsorbed water is related to the hydrophilic/hydrophobic nature of the inner surfaces. Because of the large amount of data available chiefly from infrared studies, it is possible to discriminate among three relaxing species, water molecules physisorbed in the first layer, H-bonded geminate hydroxyls and isolated hydroxyls.

3.2. Chalk

Chalk of natural origin (Champaign, France) is a pure calcite solid. The porosity ϕ, deduced from density is 15%. The specific surface area measured with krypton is $A_s = 2m^2\,g^{-1}$; in wet conditions the Young's modulus is 12 GPa.

Because of the sensitivity of calcite surfaces to temperature (possible decomposition into CaO) no high temperature dehydroxylation treatment has been given to chalk samples. Only dehydration experiments, i.e. heating at 150 °C, have been conducted, results of which are presented on Fig. 4 in reduced form. As on Vycor, during drying of a previously water-soaked sample no changes are noticeable from $X = 1.15$ down to $X = 1.05$ where a shallow maximum can be resolved in $Q^{-1}(X)$. Near $X = 1$ the large decrease in Q^{-1} is related to the increase in E in a tight manner. A maximum in Q^{-1} near the dry state is noticeable in numerous publications [5, 8]. In the case of Massillon sandstone it has been attributed by Murphy to a frequency dependence of the attenuation.

(In Murphy's resonant bar experiments as in dynamic flexural tests, the frequency varies as the Young's modulus, but this assertion has never been checked.)

3.3. Alumina

Alumina, purchased from Degussa, is a coarse grain material, 40 μm diameter, of large porosity, 25%. The BET surface area is low, $0.2\,m^2\,g^{-1}$ and agrees with the mean grain diameter according to the relation $A_s = 6/\rho d$ when only external surface of the grains is considered. Though taken from the same body, alumina samples exhibit a large variability. Young's modulus of pristine samples may differ by 40%, mass losses on heating at 800 °C range from 4×10^{-3} to 2×10^{-2} with a peak at 350 °C in the thermogram. It is believed that the initial hydroxide content varies from sample to sample, though X ray analysis failed to reveal any of the intermediate alumina phases ending to α alumina. Results presented thereafter refer to hydroxylated alumina.

Alumina can withstand high temperature annealing without suffering decomposition, only dehydroxylation of surface species is expected on heating. After a high temperature vacuum annealing, the sample is first allowed to adsorb water vapour from the laboratory air while X, Q^{-1} and E are recorded. After equilibration at the laboratory ambient, the sample is soaked into distillated water up to saturation. X, Q^{-1} and E are then continuously recorded during drying of the sample down to the $X = 1$ value. The influence of high temperature annealing on $E(X)$ is presented in Fig. 5, while its action on $Q^{-1}(X)$ is displayed on Fig. 6. Table II represents the air equilibrated Q^{-1} values as a function of the annealing temperature T_{an}.

The results on Young's modulus presented in Fig. 5 are similar to those obtained on chalk: no changes in the liquid state and huge variations near the dry state. Also apparent on the figure, a large decrease in Young's modulus in the dry state as a function of the temperature of annealing T_{an}.

As on calcite $Q^{-1}(X)$ exhibits a large plateau in the wet state (Fig. 6) and a dramatic decrease near the dry state. In the vicinity of the dry state a maximum is apparent only after a slight annealing (250 °C). In Table II, from the results in the second row, it can be seen that, contrarily to Vycor, high temperature annealing is needed to obtain low damping on alumina. Changes in damping upon adsorption from the laboratory air are described by comparing results in row 4 and row 2. The corresponding change in mass ΔX is as low as $2 \times 10^{-4}\,g\,g^{-1}$ and the transient data, not presented here, fit a linear relationship, already observed on other systems [2, 9]. Comparison of the results in the third and in the fourth row shows that some rehydroxylation has taken place during the experiment which involves soaking of the sample in liquid water.

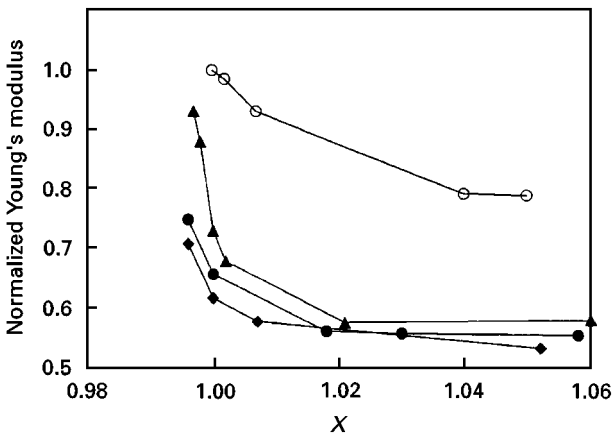

Figure 5 Normalized Young's modulus of alumina as a function of the water content during drying, after annealing at the indicated temperatures. (○) 150 °C; (▲) 250 °C; (●) 350 °C; (◆) 700 °C.

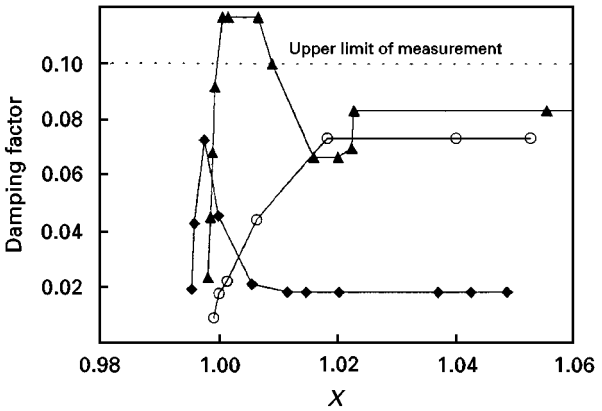

Figure 6 Damping factor of alumina as a function of the water content during drying, after annealing at the indicated temperatures. (○) 150 °C; (▲) 250 °C; (◆) 700 °C.

TABLE II Damping factor of an alumina sample in the dry and air equilibrated states after annealing at characteristic temperatures.

T_{an}	25	250	350	450	700
Q^{-1} dry after outgassing	0.0098	0.0071	0.011	0.0083	0.0038
Q^{-1} dry after soaking	0.0098	0.021	0.028	0.020	0.025
Q^{-1} equilibrated at ambient temperature	0.028	0.019	0.014	0.011	0.011

3.4. Magnesia

The experiments performed on alumina have been duplicated on magnesia, the results of which are presented on Figs 7 and 8. The general trends of alumina are followed by magnesia but significant departures can be resolved. $Q^{-1}(X)$ does not exhibit maxima as in Fig. 6 on alumina. The changes in $Q^{-1}(X)$ and $E(X)$ as a function of the annealing temperature are not monotonic ones. A maximum in $E(X)$ and a minimum in $Q^{-1}(X)$ are apparent at an annealing temperature of 450 °C. The 700 °C $Q^{-1}(X)$ curve is shifted up near the 25 °C $Q^{-1}(X)$ curve and the corresponding $E(X)$ curve is concave rather than convex towards the X axis. Since $E(X)$ and $Q^{-1}(X)$ have been linked to the state of hydroxylation of the surface at the time of measurement, it means that the rehydroxylation of magnesia, previously degassed at 700 °C, occurs on the time of measurement after water soaking. Slight rehydroxylation have been noticed on alumina. In Table II the

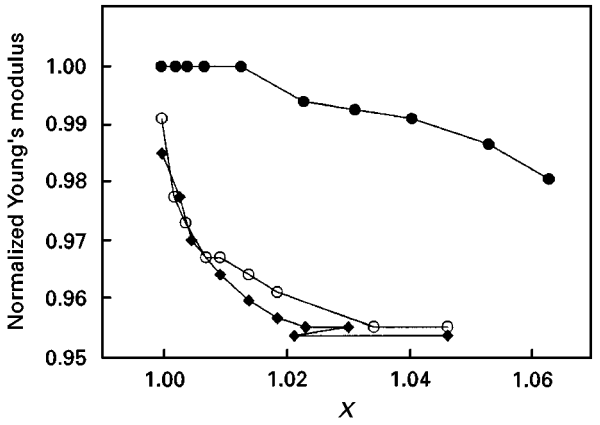

Figure 7 Normalized Young's modulus of magnesia as a function of the water content during drying, after annealing at the indicated temperatures. (●) 450 °C; (○) 150 °C; (◆) 750 °C.

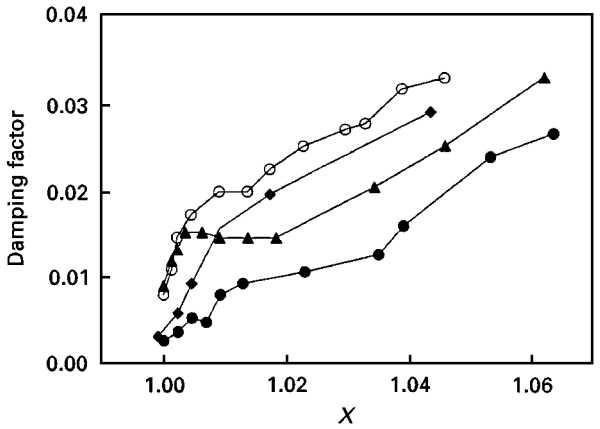

Figure 8 Damping factor of magnesia as a function of the water content during drying, after annealing at the indicated temperatures. (○) 150 °C; (▲) 300 °C; (●) 450 °C; (◆) 700 °C.

damping factor of an air equilibrated alumina sample is higher after water soaking than on adsorption from the laboratory air. On magnesia the whole $Q^{-1}(X)$ curve is shifted upwards. On the contrary silica surfaces are not prone to hydroxylation upon measurement. It is then suggested that the rates of hydroxylation R^{hydro} of heat treated oxides are as follows $R^{\text{hydro}}_{\text{Magnesia}} > R^{\text{hydro}}_{\text{Alumina}} > R^{\text{hydro}}_{\text{Silica}}$. This classification is widely accepted [10].

3.5. Graphite

Oxygen-free graphite is naturally hydrophobic and is not wetted by water. The angle of contact is near 180°, there is no noticeable mass uptake upon immersion of a porous graphite sample into liquid water and it adsorbs only a small amount of water from the gas phase at 60% RH (0.2 mg g^{-1}). Graphite can be made hydrophilic by prolonged heat treatment at 550 °C in air and/or by wet treatment in diluted (30% in volume) nitric acid. During these oxidative treatments, $(1\,1\,\bar{2}\,0)$ and $(1\,0\,\bar{1}\,0)$ prismatic planes are formed at the expense of the basal plane. These edge planes chemisorb oxygen extensively during oxidation at 550 °C [11]. At room temperature water vapour

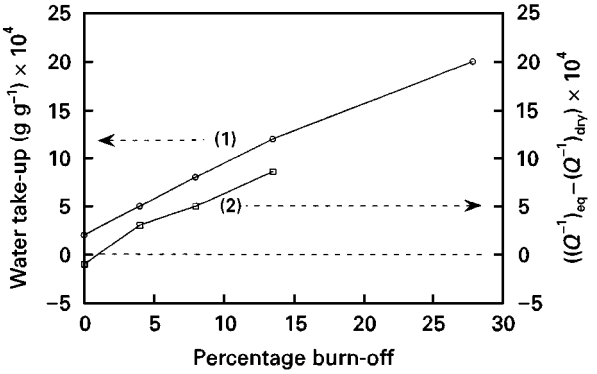

Figure 9 Amount of water vapour (1), measured by gravimetry in g g^{-1}, adsorbed on a porous graphite sample after the burning off of graphite in air at 550 °C and subsequent changes in the damping factor (2). On the right hand side of the figure the plotted parameter is $((Q^{-1})_{eq} - (Q^{-1})_{dry})$ where $(Q^{-1})_{eq}$ refers to a sample equilibrated with the ambient atmosphere and $(Q^{-1})_{dry}$ refers to a sample in the dry state after gentle degassing at 150 °C.

physisorbs on these oxygenated surfaces by H-bonding. Water can be desorbed by heating at 150 °C while chemisorbed oxygen is desorbed by heating under vacuum at 800 °C [11, 12, 13], so that the extent of water vapour and oxygen adsorptions can be measured by thermogravimetry if the nature of the high temperature desorption products, either carbon monoxide or carbon dioxide, is known.

In Fig. 9 the amount of water vapour physisorbed at 22 °C and 60% RH is plotted against the burn-off of graphite. At the exception of a small residual uptake (0.2 mg g^{-1}) the adsorption depends linearly on the amount of burn-off, which indicates that the creation of edge planes is rate limiting. Knowing the mass loss upon vacuum desorption at 800 °C, the number of water vapour molecules physisorbed per chemisorbed oxygen atom can be calculated. The experimental value, 0.36, assuming desorption as carbon dioxide, compares well with 0.8, the value given by Walker and Janov under similar conditions on Graphon, a highly oriented graphite powder [11].

As burn-off proceeds, porosity of the sample increases, leading to a decline in the Young's modulus of the sample. The experimental results, presented in Fig. 10 can be fitted by the phenomenological relationship

$$E = E_0 \exp(-b\phi) \tag{5}$$

where the numerical value of the fitting parameter b is 5.5. The rather high value of the constant b proves that the oxidation reaction creates a harmful sheet-like porosity. For instance, creation of spherical cavities would lead to $b \neq 2$ [14]. Furthermore, the krypton isotherms, obtained on samples at different burn-off levels, presented in Fig. 11 show the gradual disappearance of the $p/p_0 = 0.4$ step which is indicative of the formation of the second monolayer on the homogeneous $(0\,0\,0\,1)$ basal plane of graphite [15]. The same rounding-off of the second step has been observed by Goffinet during ozone treatment of P33 carbon [16]. Fine details in the first ascending branch

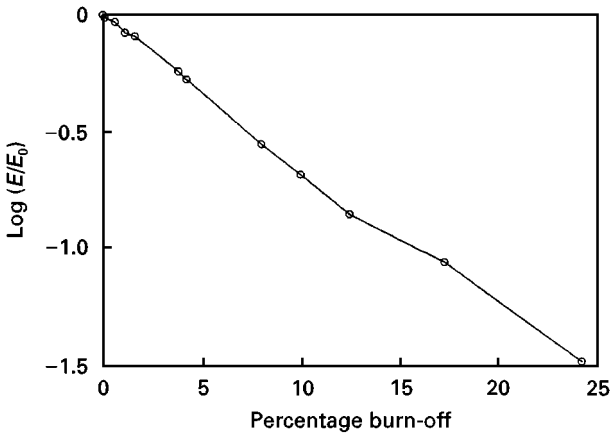

Figure 10 Young's modulus of a graphite sample at different burn-off levels.

at $p/p_0 < 10^{-2}$ can also be interpreted as a roughening of the surface but will not be discussed at length here. Oxidation, either dry or wet, can be described as the attack of the basal, hydrophobic, plane of graphite at the benefit of the prismatic planes. These highly corrugated planes can chemisorb oxygen on the so-called edge sites. At room temperature water vapour can form H-bonds with the polar oxygenated sites such as carbonyls or carboxyls groups. At the highest burn-off investigated (28%), assuming that each edge site chemisorbs one water molecule at RH = 60%, instead of the value 0.36 quoted above, one can calculate that prismatic planes are approximately of the same extension than the basal plane, $6\,m^2g^{-1}$. On the average there is one hydrophilic site per hydrophobic site, this value is rather high, a more generally accepted value lies near 0.1 [13]. As the sample turns to be hydrophilic by the oxidative treatment, its damping behaviour during water vapour adsorption changes. Instead of decreasing slightly the damping factor as on virgin, non-oxygenated samples, water vapour adsorption increases it on oxygenated ones.

In Fig. 9, beside the water up-take, the changes in damping factor upon adsorption up to equilibrium with the laboratory atmosphere (RH = 60%) is plotted as a function of the burn-off. It is apparent that the increase in the damping factor is related to the amount of water adsorption, itself related to the chemisorption of oxygen, in a very tight manner. On non-oxygen-treated samples a small water vapour adsorption ($0.2\,mg\,g^{-1}$) can be measured, but this adsorption is accompanied by a definite decrease in the damping factor (the first point of curve (2) in Fig. 9 has a negative ordinate). It is conjectured that, instead of H-bonding, this shallow adsorption results from van der Waals' forces, not operative in the damping process. This result is at variance with the results obtained on oxides, silica [1], alumina and magnesia where, even on the most dehydroxylated surfaces, the hydrophobicity of the surfaces induced by heating dictates the rate of adsorption from the gaseous phase dX/dt but not the rate of change in damping dQ^{-1}/dX. It is felt that high temperature treated oxides are still more hydrophilic than unoxygenated graphite.

It must be stressed that heating at 800 °C under vacuum does not revert the surfaces to a fully hydrophobic situation. Water vapour adsorption is still

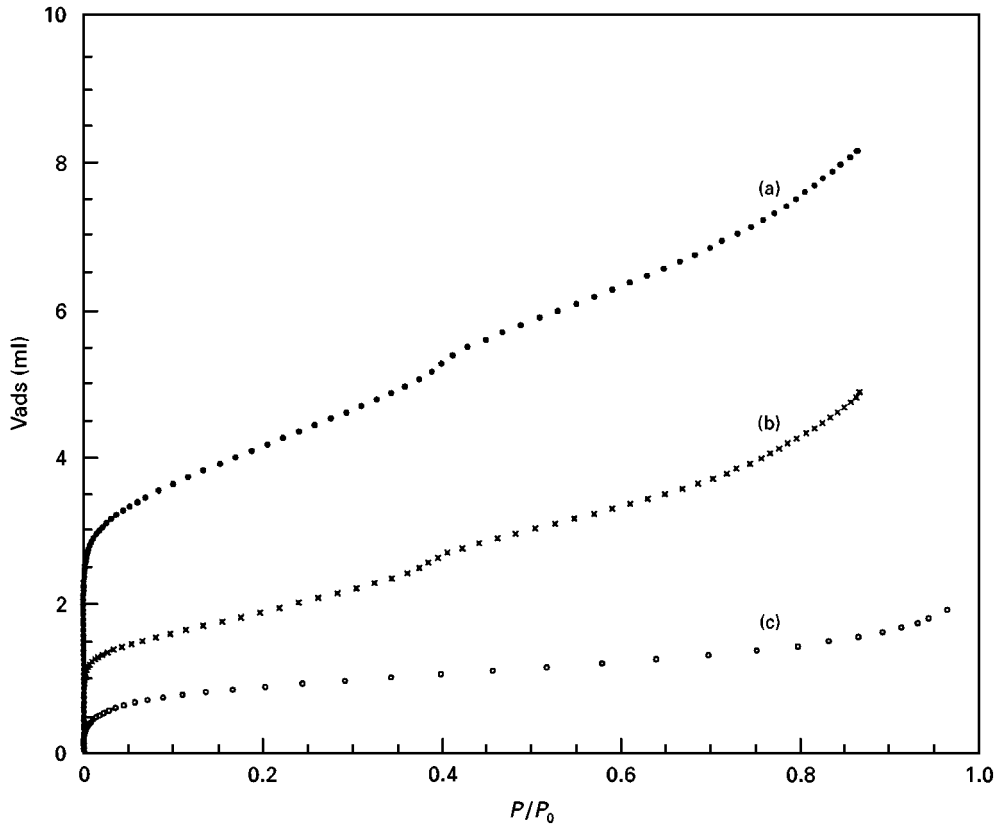

Figure 11 Krypton isotherms at 77 K on graphite oxidized at different burn-off levels. (a) 0%; (b) 4%; (c) 9.6%. Corresponding BET surface area: (a) $45\,m^2\,g^{-1}$; (b) $16\,m^2\,g^{-1}$; (c) $12\,m^2\,g^{-1}$.

TABLE III Damping factor of a graphite sample in the dry and air equilibrated states after annealing at characteristic temperatures under vacuum

	Oxygenated after 10% burn-off	Vacuum heated at 800 °C
Dry	0.010	0.0073
Equilibrated at 22 °C, 60% RH	0.014	0.0090

TABLE IV Anelastic properties of granite at various cracking rates

	Porosity	E/E_0	E_{wet}/E_{dry}	Q^{-1}_{dry}	Q^{-1}_{wet}
Pristine sample	1×10^{-3}	1	1.04	0.021	0.048
Sample heated at 450 °C	5×10^{-3}	0.45	1.16	0.027	0.159

higher than on virgin surface, however, due to the desorption of oxygen complexes, the damping factor is lower on samples degassed at 800 °C than on oxygenated ones. Though tightly bound to the substrate in strong chemisorption bonds, the oxygen complexes on graphite have damping capabilities, a situation opposite to highly bound hydroxyls on silica. A typical situation is described in Table III where the damping factor of graphite after various treatments is indicated.

3.6. Granite

Granite is a quartz-rich, multiphasic mineral from Neuvy-Bois (Vendée, France) quarry. The experiments are aimed at the characterization of the thermal cracking induced by the mismatch of the thermal expansion coefficients of the various phases. The anelastic properties are first measured in the dry and wet states, then, the same measurements are performed after a 450 °C annealing. Results are presented in Table IV.

Porosity change (4×10^{-3}) is deduced from mass gain after immersion in water, it is then an open porosity. It has a dramatic effect on the Young's modulus which cannot be taken into account by Equation 5. A more appropriate analysis would involve Budiansky's model of cracked solids [17]. Its action on damping in the dry state is small (30% increase) but much more intense in the wet state (three fold increase). As on Vycor, water adsorption stiffens the structure, $(E_{wet}/E_{dry}) > 1$. The relative enhancement is higher on cracked than on pristine samples. As a whole, experimental results on granite do agree with the H-bonding model of water on hydrophylic surfaces, a conclusion arrived at by Morlier *et al.* using velocity of sound measurements [18]. Work by Gregory [19] on Brazilian gabbro led to similar results. Heating to 750 °C causes a 40% reduction in velocity V_s on dry samples and an enhanced sensitivity to environmental conditions. He classified rocks according to $R = V_s(S_w = 100)/V_s(S_w = 0)$. $R > 1$, which contradicts Biot's theory is obtained on low porosity rocks. It is believed that this criterion is more related to the crack aspect ratio and/or to the hydrophilic character of the crack surfaces than to the overall porosity. The main conclusion relevant to this study is that thermal cracking of polyphasic rocks lowers both the Young's modulus and the quality factor Q of the materials and increases the environmental sensitivity. It is concluded that in porous materials with one solid phase, changes in the elastic constants on heating do not result from thermal cracking bur from void formation involving phase changes in the solid state at the grain contacts such as hydroxide → oxide change. This contradicts conclusions by Clark [20] and Schmidt [8] but agrees with Bourbié [21].

3.7. Mordenite

Mordenite is a high silica containing zeolite of natural origin (Hungary). Its formula is (Na_2K_2Ca)-$[Al_2Si_{10}O_{24}].7H_2O$. Water in zeolites rests essentially in the open channels of the aluminosilicate framework. In mordenite these channels have a 0.7 nm access aperture [22] and it appears that this dimension is well suited to bridge the gap between alumina where flaws of molecular dimension dictate the average behaviour and Vycor the dimension of which is 2 nm. Furthermore, in zeolites, the classical distinction between free water desorbing below 150 °C and bound water and/or hydroxyls does not hold. In zeolites, water adsorbed in molecular states desorbs at temperatures as high as 350 °C [23].

Experiments on mordenite are identical to those conducted on Vycor, the results of which are plotted in Figs 1 and 3. The corresponding results for mordenite are presented in Figs 12 and 13. During high-temperature annealing the gradual departure of the constitutive water and/or hydroxyls leads to a small but irreversible decrease in the Young's modulus as on alumina and magnesia. Because of its surface area mordenite adsorbs large amounts of water vapour from the gas phase. The increase in Young's modulus during the initial stage of hydration can be explained by H-bonding, as on Vycor. As apparent from Fig. 13, no clear distinction can be made between molecular water desorbing below 150 °C ($X > 1$) and more strongly bound species desorbing at higher temperature ($X < 1$) . The same conclusion can be drawn from the temperature dependence of the Young's modulus presented on Fig. 12. The fall in Young's modulus as a result of heating ($0.98 < X < 1$) is a mere extrapolation of the first adsorption run. In other words, only one water species is operative in mordenite whatever its temperature of desorption. This agrees with the fact that on zeolites molecularly adsorbed water desorbs at temperatures up to 350 °C [23]. Recent nuclear magnetic resonance (NMR) results tend to show that hydroxyls and water adsorbed in porous glass have the same relaxation dynamics [24]. This raises doubt about the generality of the discrimination made among the different relaxing species introduced on Vycor.

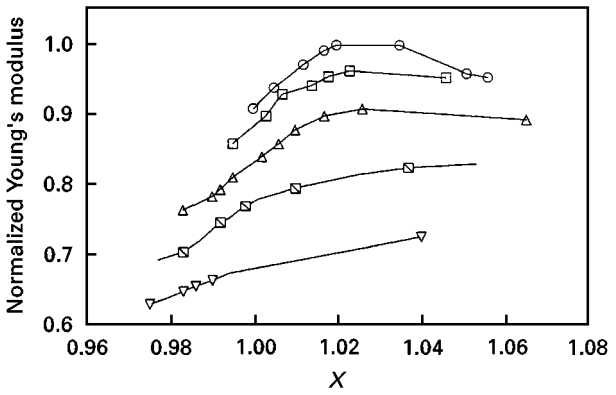

Figure 12 Normalized Young's modulus of mordenite as a function of the water content during adsorption from the laboratory air, after annealing at the indicated temperatures. (○) 150 °C; (□) 300 °C; (△) 500 °C; (▨) 700 °C; (▽) 800 °C.

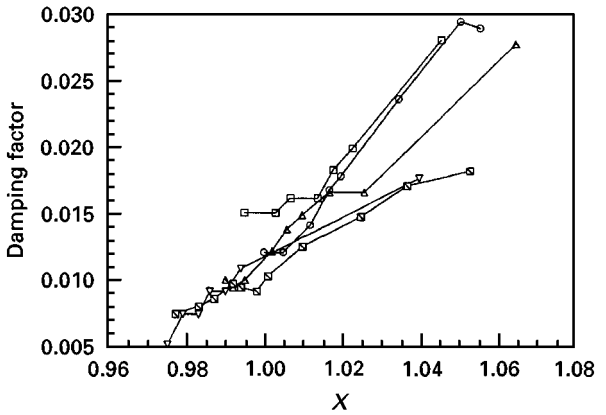

Figure 13 Damping factor of mordenite as a function of the water content during adsorption from the laboratory air, after annealing at the same temperatures as in Fig. 12.

4. Discussion

4.1. Elastic properties

On Vycor, granite and mordenite the rate of change of Young's modulus dE/dX is positive, but the magnitude of the effect is rather small. This is linked to the low spring constant of the hydrogen bond ($20\ N\ m^{-1}$) which covers the inner part of the pores. On alumina and mainly on chalk dE/dX is negative and the magnitude of the effect is much larger. The sensitivity to high temperature treatments displays also a large range of behaviours. The increase in the stiffness of Vycor by siloxane bond formation is well documented [25, 26] but this case is the only one, generally heating a material lowers its room temperature elastic constants. On alumina and to a less extent on magnesia, the decrease in Young's modulus is closely related to the hydroxide → oxide phase change. The change in specific volume associated with this transformation leads to a harmful porosity at the contact grain. In two phase minerals such as granite the mismatch of the thermal expansion coefficients creates sheet-like voids at the interface. On mordenite the decrease of the elastic constants is related to the departure of the constitutive water.

The decrease in frame moduli upon adsorption of minute amount of water has been noted by numerous authors who merely noted that this reduction is not expected from the Biot theory of porous media. An attempt to relate frame moduli reduction and water adsorption without resort to extensive chemical bond breaking has been presented by Murphy and co-workers [27] and the main lines are presented here.

According to Digby's model [28] the perpendicular and parallel stiffness of a dense packing of elastic spheres of radius R are given by

$$k_0^{\parallel} = \frac{2Ga_0}{1-\nu} \tag{6}$$

and

$$k_0^{\perp} = \frac{4Ga_0}{2-\nu} \tag{7}$$

where a_0 is the radius of contact of two spheres, G the shear modulus and v the Poisson's ratio. In Hertz theory

$$a_0^3 = \frac{3(1-\nu)RF}{8G} \tag{8}$$

where F is the normal load.

The equation for the Young's modulus is then

$$E = \frac{3(1-\phi)\psi}{20\pi R}\left(K_0^{\parallel} + \frac{3k_0^{\perp}}{2}\right) \tag{9}$$

where ψ is the coordination number, i.e. the number of contacts per grain.

In the so-called Johnson-Kendall-Roberts (JKR) theory [29], attention is paid to the van der Waals' attraction between solids through the air gap between them. This results in an enhanced radius of contact

$$a_0^3 = \frac{3(1-v)R}{8G}\{F + 6\gamma\pi R + [12\pi\gamma RF + (6\gamma\pi R)^2]^{1/2}\} \tag{10}$$

where γ is the surface energy of the solid. As adsorption is known to reduce surface energy [30, 31] a lowering in a_0 and in the moduli follows. The main ingredient of the model is the change in surface energy measured from the adsorption isotherm $\Gamma(p)$ with the Gibb's relation

$$\Delta\gamma = \gamma_0 - \gamma = RT\int_0^p \frac{\Gamma(p)dp}{p} \tag{11}$$

where $\Gamma(p)$ is the surface excess in equilibrium at the gas pressure p.

Using this model, Murphy and colleagues [27] have been able to fit the experimental results of Clark *et al.* on Coconino sandstone [2] and those of Spencer on Navajo sandstone [6], i.e. a 30% reduction in the moduli as p/p_0 increases from 0 to 1. The obtained $(E/E_0, p/p_0)$ relationship is linear, which reflects the sluggish adsorption at small p/p_0. If adsorption at small p/p_0 were more important (type I isotherm), large changes would be expected at small partial pressure because of the $1/p$ term in the Gibbs' equation. This would fit for instance the steep decrease in Young's modulus at low water content measured in this study on chalk (Fig. 4) and alumina (Fig. 5) and by Murphy [5] and Schmidt [8] on Massilon sandstone.

Reversible adsorption at room temperature, i.e. physisorption does not involve the breaking of chemical bonds. However, in porous materials, it leads generally to a weakening of the solid as shown by the lowering in the effective Young's modulus. The situation may be compared to another related field: the adsorption induced lowering of the strength of materials. The situation is described with the help of the Griffith's theory of brittle solids, the stress at rupture is

$$\sigma_r = \left(\frac{2\gamma E}{\pi c}\right)^{1/2} \tag{12}$$

where γ is the surface energy of the solid and c the length of the crack.

As adsorption proceeds the surface energy is reduced by an amount $\Delta\gamma = \gamma_0 - \gamma$ given by the Gibbs' law of adsorption (Equation 11) and σ_r is reduced in the corresponding manner. In the literature various physical situations can be found. For instance Rehbinder and Shchukin [32, 33], working with well designed magnesium hydroxide of large specific surface, observed that the experimental results follow the Griffith's equation

$$\frac{\sigma_r^2 - \sigma_{r0}^2}{\sigma_{r0}^2} = \Delta\gamma \tag{13}$$

where $\Delta\gamma$ is obtained from the adsorption isotherm $\Gamma(p)$ by Equation 11. When the adsorption isotherm cannot be determined, as in the work of Hiller on porous glass [34], one can invoke Bangham's law [35]

$$\frac{\Delta l}{l} = \lambda\Delta\gamma \tag{14}$$

where $\Delta l/l$ is the swelling of the sample during adsorption and λ a constant depending on the bulk modulus of the solid. Hiller [34] obtained linear relationship in the $(\sigma_r^2, \Delta l/l)$ plot. It is to be noted that in these experiments, (Gibbs + Griffith) criteria is fulfilled over a large range of relative pressure up to $p/p_0 = 0.45$.

On the other hand, experiments on poorly consolidated compacts, such as calcite compacts or silica compacts used in infrared studies, show a huge dependence of strength on water vapour pressure. For instance, on calcite, Dollimore and Gregg [36] obtained a 50% reduction in strength over the dry state value at 10% RH. In order to apply the above mentioned theory it is necessary to invoke a large adsorption at low RH which is indicative of a microporous solid, i.e. a type I BET isotherm. The situation is reminiscent of the large variations in Q^{-1} and E at low RH obtained on alumina in this study and by Pandit and King [37] and Murphy [5] on sandstones.

4.2. Damping properties

With the exception of chalk and alumina, which present a definite maxima in the $Q^{-1}(X)$ curve, the damping factor is a monotonic, growing function of the water content, but the magnitude of dQ^{-1}/dX differs considerably from material to material. The variation interval can be swept while ΔX is as low as $2\times10^{-4}\,g\,g^{-1}$ on alumina in this study and even $10^{-4}\,g\,g^{-1}$ in sandstone [37] or a few $10^{-2}\,g\,g^{-1}$ in Vycor or mordenite in this study and as noted by previous authors [38] these data cannot be fitted by a single model.

As a general rule dQ^{-1}/dX is small if dE/dX is positive (Vycor, mordenite) and dQ^{-1}/dX is large when dE/dX is negative (alumina, chalk). This is an extension of Clark's conclusion who noted that "the rocks with the largest Q^{-1} have the largest (negative) changes in velocity (i.e. in moduli) as $p/p_{0(H_2O)}$ is varied" [20]. Also apparent from her work the fact that the higher the Q_0^{-1}, the steeper the subsequent change in Q^{-1} as $p/p_{0(H_2O)}$ is varied. This leads her to suspect the presence of clay softened by chemical interaction with water (water intercalation) at the contact between grains, a hypothesis that has been refuted later [21]. A goal of this paper is to explain water-induced anelasticity on the basis of sole physical interactions, without resort to chemical bond breaking concept. Only van der Waals' interactions and hydrogen (bonding/breaking) need to be invoked in the discussion.

The H-bond breaking mechanism considered by Spencer [6], Tittmann [9] and Bourbié *et al.* [21] implies that the damping varies with the number of adsorbate–substrate bonds to be broken i.e. $Q^{-1} = Q_0^{-1} + k_1[OH][H_2O]$.

In this analysis the second term of Equation 1 is omitted and according to this model Q^{-1} levels off at the monolayer coverage. Two obvious consequences arise. First, keeping the chemistry constant, the attenuation factor must be directly linked to the specific surface area of the solid as measured for instance by the BET method. Secondly, for a given material, damping must vary with the water vapour partial pressure in the same manner as $[H_2O]$, the water coverage determined on an adsorption isotherm. These assumptions are often not verified. For instance Massilon sandstone of low specific surface $A_s = 1\,m^2\,g^{-1}$ has a quality factor at saturation $Q_{wet} = 20$ while Vycor, another silicate with $A_s = 200\,m^2\,g^{-1}$ exhibits $Q_{wet} = 200$.

On most materials when equilibrium experiments are performed Q^{-1} levels off at partial pressure as low as 0.1 [37] while completion of the first monolayer takes place at $p/p_0 = 0.4$. In transient experiments, Pandit and King [37] found a mass increase at saturation as low as $10^{-4}\,g\,g^{-1}$, a value similar to those obtained in this paper on alumina ($2\times10^{-4}\,g\,g^{-1}$).

The leveling off in the $Q^{-1}(X)$ curve at the completion of the monolayer has soon been noted by various authors [2, 5, 38, 39]. Damping is a true surface mechanism and the H-bond breaking mechanism is relevant in this situation. However detailed analysis shows that the completion of the statistical monolayer occurs at $p/p_0 = 0.4$ whilst the levelling off of the damping process occurs frequently at $p/p_0 = 0.1$. Furthermore, as noted by Murphy [5] and Bourbié *et al.* [21] the amount of water involved in the process depends linearly on the specific surface area and it is hard to conceive how a single process can account for a one hundred change in efficiency. The success of the monolayer correlation is fortuitous and hides two

physically different situations. On smooth surfaces H-bond breaking mechanism, thereafter named mode II is operative. Mode I, operative on rough surfaces is a kind of boundary lubrication process and requires further comments.

4.2.1. Hydrophilicity index

It appears that the anelastic properties–water adsorption relationship is dominated by a small fraction of the surface area of the solid which is hardly measurable by conventional methods. It is well known that the water vapour surface area may be larger than the N_2 or Kr surface area by a factor of ten [10]. This is related to the wedging action of water on hydrophilic interfaces. As water adsorption of hydrophilic surfaces reduces surface energy by a large amount, the spreading pressure $\pi = \gamma_0 - \gamma$ tends to create new internal surfaces leading for instance to swelling of the solid or to low pressure hysteresis in isotherm determination. Since these processes modify the anelastic properties of the material it is of interest to define a hydrophilicity index β as the ratio of the water surface area measured at $p/p_0 = 0.6$ to the conventional BET surface area measured with Kr. This index can be considered as an indication of the health of materials, crack-free materials, as Vycor, have $\beta = 1$ whether they are hydrophilic or not. On the contrary, poorly cemented granular solids prone to swelling, exhibit $\beta > 1$. For instance extensive ball milling of calcite has been shown to increase β from 1.2 to 10 [40]. From results gathered in Table V it is seen that the case $\beta < 1$ corresponds to mode II of water interaction, whilst the case $\beta > 1$ corresponds to mode I.

On graphite, because of its low hydrophilicity, changes in Q^{-1} upon adsorption of water vapour are not large, the results presented on Fig. 9 correspond to a relative change of 30%. On the contrary, a tenfold increase may be noticed on oxides [8, 37].

Porous media can be classified in two classes according to pore shape criterion. The first class, including Vycor and mordenite, is characterized by smooth pores with large radius of curvature. As a consequence of the mode of elaboration, (spinodal decomposition for Vycor, natural zeolitization for modernite) the solid skeleton is rigid and does not include weak contact zones and/or harmful flaws. The second type of materials includes for instance compacted silica powder used in i.r. studies, compacted calcite used as writing chalk and all poorly sintered ceramics such as alumina or magnesia used in this study. These materials contain large contact zones of ill-defined crystallographic order analogous to grain boundaries in metals, flaws of atomic dimension, badly cemented grain contacts and other deleterious defects. H-bonding model has proved to be a valuable tool to interpret the increase in stiffness of Vycor [1], the same calculus can be applied on mordenite. The hydrophobic action of high temperature annealing is reflected in the lowering of dE/dX which can be noted either on Vycor or on mordenite, the same model applies to damping.

Type I adsorption in microporous solids frequently follows the Gurvitsch rule i.e. when expressed as a volume of a liquid by use of the normal liquid density, the amount adsorbed at saturation on a given solid is the same for various adsorbates. This is taken as a proof that in micropores, adsorbates are in a liquid state even if the pores are few molecular diameters wide. In numerous solids, water induced attenuation saturates as soon as p/p_0 reaches 0.1 [5, 37] and does not change upon immersion. This is in agreement with the microporous solid model of adsorption: attenuation is dominated by liquid entrapped in fine pores saturated at $p/p_0 < 0.1$. Even if it is recognized that mode II results from a drastically different mechanism of adsorption, leading to type II isotherm, it does not tell anything about the mechanism of attenuation. In a first attempt, it is of interest to consider if the H-bond breaking model is still valuable.

In this study where the specimens are excited in flexural vibration the macroscopic strain is small (10^{-6}) and at first glance the H-bond breaking model would not be operative because H-bonds experience only the bottom of the potential well. Microscopically, the strain is much larger at singularities such as apex of flaws, regions of high curvature etc. Even if the strain is too small to break elastic H-bonds, these bonds experience non-harmonic region of the potential well, leading to mechanical dissipation. Roughness of the internal surfaces at the atomic level appears as a key parameter in the problem. It is obvious that in solids exhibiting type I isotherm, H-bond mechanism is much more efficient than on smooth, mesoporous surfaces exhibiting type II isotherm. The challenge is to account for a 100-fold ($10^{-4}\,g\,g^{-1}$ [37] versus $10^{-2}\,g\,g^{-1}$ [1]) change in efficiency. For instance, experimentally, a threefold enhancement over natural calcite has been obtained by using poorly compacted, artificial chalk which is believed to contain a large number of non-cemented contacts.

4.2.2. Maximum in the $Q^{-1}(X)$ curve

Finally, the sole phenomenon still to be explained is the maxima in the $Q^{-1}(X)$ curve encountered on alumina and chalk. As damping is expected to be a fluid flow mechanism, X is not a well-suited parameter and S_w, the pore fluid filling factor is preferred. In this work and in other studies [5, 8] where this peak is apparent, it is located at $S_w = 0.2$, which is the symmetrical of $S_w = 0.8$ where numerous peaks have been resolved [5, 21]. In every case, the attenuation peak is associated with a huge change of the modulus [5, 8], which is taken as a roughness effect. On alumina, the peak is resolved only after high temperature heating which cancels the H-bond breaking mechanism.

In order to account for the changes in Q^{-1} Walsh [41] and Gordon and Davis [42] developed a surface

TABLE V Hydrophilicity index β of some minerals

Material	Graphite	Vycor	Chalk	Magnesia	Alumina
b value	$0.013 \rightarrow 0.5$	~ 1	5.1	6.6	6.6

friction model. They recognized that in fissured solids anelastic properties are dominated by flaws. As water adsorption decreases sliding friction at surfaces [43] it allows the relative motion of the nearly contacting opposite faces of the flaws, thus increasing the mechanical losses. Walsh obtained the following formula

$$Q^{-1} = \frac{1}{15}\frac{E}{E_0}c^3 n^3 h(f) \tag{15}$$

where E/E_0 is the ratio of effective and intrinsic moduli, c and n, respectively, the length and density of nearly contacting flaws and $h(f)$ a function of the friction coefficient f exhibiting a maximum at a given f. Such a micromechanical model can afford for the existence of a maximum. The main criticism addressed to it is that, in order to account for the constancy of Q^{-1} upon hydrostatic pressure changes, it requires an unrealistic density of cracks.

Schmidt *et al.* [8] considered, in clay bearing rocks, the bound water $\Leftrightarrow$ free water equilibrium. As the dielectric losses peak at 10^{10} Hz in bound water instead of 10^{12} Hz in free water, application of the Debye formula $\tau = 8\pi\eta a^3/2kT$ where τ is a dielectric relaxation time, η the viscosity and a the atomic radius, shows that bound water is 100-fold more viscous than free water. At saturation free and bound water are physically in contact, the equilibrium is established and free water influences bound water, so that viscosity is low. Below a critical water filling factor S_B, determined from NMR experiments, bound water is not stable and the viscosity drops rapidly. According to Schmidt the clay content of the rocks is a key parameter since it is known that water self-organizes at clay surfaces. This conclusion has been largely dismissed since such maxima have been observed on no clay bearing rocks [5].

On Coconino sandstone, Murphy [44] considered the squirt flow from low aspect ratio pores to larger pores. At saturation the flow is restricted for the larger pores are filled, in the dry state obviously no transit can take place.

Blandamer [45] reviewed the acoustic properties of aqueous mixtures and considered plot A, i.e. the ratio α/ν^2 where α is the absorption coefficient and ν the frequency, versus composition x^2. These plots exhibit a zone of intense absorption named PSAC (peak sound absorption coefficient) if the system presents a positive deviation from thermodynamic ideality, $\Delta G^E > 0$. When ΔG^E is negative, however PSAC can occur if the mixing character of the co-solvents can be called hydrophilic. He also noted that PSAC develops near T_C, the critical temperature of the mixture. He concluded that the shape of plot A can be used as an indication of the hydrophilic/hydrophobic character of the organic co-solvent.

Keeping this analysis of the literature in mind, it is fruitful to make some comments.

(i) Maxima on the $Q^{-1}(S_w)$ on alumina is apparent only after extensive dehydroxylation of the surfaces which renders them more or less hydrophobic, the hydrophilicity of chalk is not known.

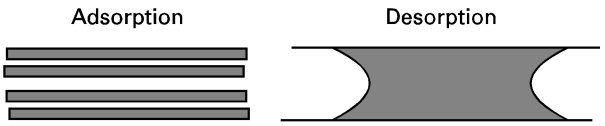

Figure 14 Schematic drawing of the adsorption layer in a cylindrical pore. (a) During adsorption from the laboratory air. (b) During drying of a previously water soaked sample.

(ii) This maxima is associated with a large change in the Young's modulus, itself related to the roughness of the surface at the atomic scale.

(iii) It has been observed only during drying, in the literature no report of this maximum during imbibition has been found.

Fluid flow, i.e. differential motion of the fluid and of the solid is closely related to the wetting behaviour of the fluid and two limiting cases arise. If wetting is perfect, $\theta = 0$, the fluid sticks to the wall and losses are minimized. If non-wetting conditions prevail ($\theta = 180^\circ$) the liquid drops float over the surface and viscous losses are expected also to be low. Furthermore, because of the Laplace pressure $p - p_0 = 2\gamma/r$, the liquid inside of the meniscus experiences a negative pressure, as in critical conditions. It is worthy of interest to note that no maximum has been detected during imbibition. In systems where capillary hysteresis exists, during adsorption the liquid film grows in a layer-by-layer mode and cannot experience Laplace pressure. On the contrary, during desorption, the liquid–air interface keeps the same radius of curvature and negative pressure can develop inside the fluid phase. The physical situation is displayed in Fig. 14.

It appears that the maximum in sonic or ultrasonic attenuation is related to a particular organization of the liquid inside the porous space. However, no water structure formers such as clay platelets or solvating ions (Ca^{2+}, K^+) are necessary. This dissipative structure results from the departure of the equilibrium conditions that exist at saturation. The situation may be compared to the damping of waves at the surface of liquids by Marangoni effect, damping feels surface modification earlier than defect modulus does. This is a general phenomenon, for instance in the case of damping of surface waves on liquids by surfactants, $Q^{-1}(A)$ is much more structured than the corresponding $\pi(A)$ curve, where $\pi(A)$ is the surface pressure and A is the surface per molecule [46].

At low solute concentration the driving term $\gamma_{dyn} - \gamma_{stat}$, where γ_{dyn} is the surface tension of the disturbed surface and γ_{stat} that of the undisturbed surface, is low. At high bulk concentration the equilibrium surface concentration is re-established before the restoring forces can act. Clearly, this can lead to a peak in the damping versus concentration curve. The governing process, which can introduce phase lag in the stress-strain relation, is the diffusion from the bulk of the liquid to the surface. In the case under study surface diffusion is operative and the governing parameter is the mean square displacement $\langle x \rangle$. The Einstein relation $\langle x \rangle^2 = 2Dt$ links the surface diffusion coefficient D to the time t. Assuming a liquid like

behaviour of the adsorbate, D may be taken equal to $10^{-9}\,m^2\,s^{-1}$, the coefficient of self-diffusion of bulk water [47] and $\langle x \rangle = 10^{-9}\,m$, the width of microscopic cracks considered to be effective, the diffusion time is $10^{-9}\,s$. According to this description, at saturation, the equilibrium is established by surface diffusion in the sonic and even the ultrasonic range in a time smaller than the period of the motion. This explains that dispersion is rarely observed in damping. A description of the diffusing species (bound versus free water, H-bonded versus non H-bonded water) is still a matter of debate and cannot be solved here.

The physical situation is reminiscent to that prevailing in the so-called mechano-sorption of wood and other polymeric materials [48–50]. It is found that changes in RH during either static or dynamic measurements enhance the viscoelastic properties of these hygroscopic materials. The mode of coupling of the adsorbate with the stress field of the solid is supposed to be through hydrogen bonding. As the H-bonded surface network undergoes reorganization as the total moisture content changes, one can imagine that particular configurations out of equilibrium are strongly energy-dissipative. This can account for the drying rate sensitivity observed in an irreproducible manner (and so not reported) in this study. No explanations beyond those put forward in this paper are offered by the authors [48–51].

As a final remark, the system bears some similarities with differential scanning calorimetry (DSC) experiments [52, 53]. As S_w decreases, exothermic peaks of ice crystallization frequently exhibit negative shifts in temperature and structures not explainable by the Kelvin relation [54]. In this case also, it is suspected that, at intermediate S_w, energy barriers arise between water species located in different local environments, which leads to compartmentalization. It appears that non-equilibrium mechanisms are important at intermediate S_w and may be invoked to explain a wide class of phenomena, especially enhanced attenuation. At saturation, equilibrium conditions prevail and small losses, either dielectric or mechanical, are expected.

5. Conclusions

In healthy porous solids with a rigid framework, water H-bonds to surface hydroxyls and acts as a stiffener of the structure. This permits a clear distinction between hydrophilic and hydrophobic surfaces. In cracked solids, the wedging action of water increases crack length and leads to a considerable change in the elastic moduli. Application of the Gibbs' equation coupled with a micromechanical model of cohesion allows for a qualitative interpretation of the experimental results.

Attenuation is a growing function of the water content. Experiments on graphite as a function of the hydrophilic character of the substrate provide an enlightening proof of the H-bond breaking mechanism. With regards to damping efficiency, no clear distinction can be made among water molecules in the first layer and low temperature desorbing hydroxyls. It is found that the monolayer correlation, commonly advanced in the literature, must be revisited. Detailed analysis of the shape of water or krypton isotherm, leading to a precise description of the pore structure, is much more important than the mere value of the BET surface area. The maximum in Q^{-1} encountered during drying of mildly hydrophilic materials has been interpreted in the general context of phase changes of liquids in porous media. Clearly more experimental results are desirable in order to work out a precise model.

Acknowledgements

The authors are indebted to Mrs. J. J. Royer and C. Le Carlier de Veslud, at Centre de Recherches Pétrologiques et Géologiques (CRPG), Vandœuvre-les-Nancy, for the gift of mineral samples and for many fruitful discussions.

References

1. J. LEPAGE, A. BURNEAU, G. GUYOT and G. MAURICE, *J. Non-Cryst. Solids* **217** (1997) 11.
2. V. A. CLARK, B. R. TITTMANN and T. W. SPENCER, *J. Geophys. Res.* **85** (1980) 5190.
3. J. C. DOUKHAN, *J. Phys. III France* **5** (1995) 1809.
4. J. C. BRICE, *Rev. Mod. Phys.* **57** (1985) 105.
5. W. F. MURPHY III, *J. Acoust. Soc. Amer.* **71** (1982) 1458.
6. J. W. SPENCER, Jr., *J. Geophys. Res.* **86** (1981) 1803.
7. T. BOURBIÉ and B. ZINSZNER, *ibid.* **90** (1985) 11524.
8. E. J. SCHMIDT, D. VO-THANH, A. NUR and B. AULD, unpublished Stanford University Research Paper. Available from the authors upon request. This report is largely cited in [21].
9. B. R. TITTMANN, V. A. CLARK, J. M. RICHARDSON and T. W. SPENCER, *J. Geophys. Res.* **85** (1980) 5199.
10. S. G. GREGG, K. S. W. SING, in "Adsorption, surface area and porosity" (Academic Press, London, 1982) p. 274.
11. P. L. WALKER Jr and J. JANOV, *J. Colloid Interface Sci.* **28** (1968) 107.
12. B. RAND and R. ROBINSON, *Carbons* **15** (1977) 257.
13. F. H. HEALEY, YUNG-FANG YU and J. J. CHESSICK, *J. Phys. Chem.* **59** (1955) 399.
14. R. W. RICE, *J. Mater. Sci.* **31** (1996) 1509.
15. A. THOMY, X. DUVAL and J. RÉGNIER, *Surf. Sci. Rep.* **1** (1981) 1.
16. P. GOFFINET, Thesis, Nancy (1972).
17. B. BUDIANSKY and R. J. O'CONNELL, *Int. J. Solid Structures* **12** (1976) 81.
18. P. MORLIER, *Revue d'Acoustique* **64** (1983) 49.
19. A. R. GREGORY, *Geophysics* **41** (1976) 895.
20. V. A. CLARK, T. W. SPENCER and B. R. TITTMANN, *J. Geophys. Res.* **86** (1981) 7087.
21. T. BOURBIÉ, O. COUSSY and B. ZINSZNER, in "Acoustique des milieux poreux" (Editions Technip, Paris, 1986) ch. 5.
22. R. M. BARRER, in "Zeolites and clay minerals as sorbents and molecular sieves" (Academic Press, London, 1978) p. 70.
23. W. A. DEER, R. A. HOWIE and J. ZUSSMAN in "Rock-forming minerals" vol 4 Framework Silicates (Longmans, London, 1963) p. 351.
24. K. OVERLOOP and L. VAN GERVEN, *J. Magn. Res.* **A 101** (1993) 147.
25. T. A. MICHALSKE, B. C. BUNKER and K. D. KEEFER, *J. Non-Cryst. Solids* **120** (1990) 126.
26. B. J. J. ZELINSKI, L. A. SILVERMAN and D. R. UHLMANN, *ibid.* **82** (1986) 349.
27. W. F. MURPHY, III, K. W. WINKLER and R. L. KLEINBERG, *Geophys. Res. Lett.* **11** (1984) 805.
28. P. J. DIGBY, *J. Appl. Mech. ASME* **28** (1982) 803.
29. K. L. JOHNSON, K. KENDALL and D. ROBERTS, *Proc. Roy. Soc.* **A324** (1971) 301.
30. G. A. PARKS, *J. Geophys. Res.* **89** (1984) 3997.

31. M. L. COHEN in Proceedings of the AIP Conference 154, Physics and Chemistry of Porous Media II, Ridgefield, CT, 1986, edited by J. R. Banavar, J. Koplik and K. W. Winkler (American Institute of Physics, New York, 1987) p. 3.
32. E. D. SHCHUKIN, M. V. DUKAREVICH, S. I. KONTOROVICH and P. A. REHBINDER, *Dokl. Akad. Nauk. SSSR* **167** (1966) 1109.
33. P. A. REHBINDER and E. D. SHCHUKIN, in "Progress in surface science" vol. 3 (Pergamon Press, Oxford, 1973) p. 97.
34. K. H. HILLER, *J. Appl. Phys.* **35** (1964) 1622.
35. P. J. SERADA and R. F. FELDMAN, in "The solid–gas interface" vol. 2 (Marcel Dekker, New-York, 1967) ch. 24.
36. D. DOLLIMORE and S. J. GREGG, *Research* (*London*) **11** (1958) 180.
37. B. I. PANDIT and M. S. KING, *Can. J. Earth Sci.* **16** (1979) 2187.
38. J. R. BULAU, B. R. TITTMANN, M. ABDEL-GAWAD and C. SALVADO, *J. Geophys. Res.* **89** (1984) 4207.
39. W. F. MURPHY, III, *ibid.* **89** (1984) 11559.
40. R. B. GRAMMAGE and S. J. GREGG, *J. Colloid Interface Sci.* **38** (1972) 118.
41. J. B. WALSH, *J. Geophys. Res.* **71** (1966) 2591.
42. R. B. GORDON and L. A. DAVIS, *ibid.* **73** (1968) 3917.
43. T. E. FISHER and H. TOMOZAWA, *Wear* **105** (1985) 29.
44. W. F. MURPHY, III, K. W. WINKLER and R. L. KLEINBERG, *Geophysics* **51** (1986) 757.
45. M. J. BLANDAMER, in "Water. A comprehensive treatise" vol. 2 edited by F. Franks (Plenum Press, New York 1975) ch. 9.
46. W. D. GARRET and W. A. ZISMAN, *J. Phys. Chem.* **74** (1970) 1796.
47. S. S. DUKHIN, G. KRETZSCHMAR and R. MILLER, in "Dynamics of adsorption at liquid interfaces" (Elsevier, Amsterdam, 1995) p. 108.
48. P. R. EBRAHIMZADEH and J. KUBAT, *J. Mater. Sci.* **28** (1993) 5668.
49. *Idem.*, *ibid.* **32** (1997) 4227.
50. D. G. HUNT, *ibid.* **19** (1984) 1456.
51. A. MÅRTENSSON and S. THELANDERSSON, *Wood Sci. Technol.* **24** (1990) 247.
52. N. MURASE, K. GONDA and T. WATANABE, *J. Phys. Chem.* **90** (1986) 542.
53. C. L. JACKSON and G. B. McKENNA, *J. Chem. Phys.* **93** (1990) 9002.
54. G. K. RENNIE and J. CLIFFORD, *J. Chem. Soc. Faraday. Trans.* **I 73** (1977) 680.

Received 4 November 1996
Accepted 5 February 1998